NASA TECHNICAL MEMORANDUM

NASA TM X-67805

NASA TM X-67805

FEASIBILITY STUDIES ON AN AUXILIARY PROPULSION SYSTEM USING MPD THRUSTERS

by James A. Burkhart and George R. Seikel
Lewis Research Center
Cleveland, Ohio

TECHNICAL PAPER proposed for presentation at
Seventh Propulsion Joint Specialist Conference sponsored by
the American Institute of Aeronautics and Astronautics
Salt Lake City, Utah, June 14-18, 1971

FEASIBILITY STUDIES ON AN AUXILIARY PROPULSION SYSTEM USING MPD THRUSTERS

James A. Burkhart and George R. Seikel
National Aeronautics and Space Administration
Lewis Research Center
Cleveland, Ohio

Abstract

A low-power MPD thruster with a downstream cathode has previously demonstrated a thrust efficiency adequate for use in auxiliary propulsion systems. Other desirable features for such an application were therefore explored. Thrust vectoring with a skewed coil arrangement was found to be feasible. Operation with a single power supply was also demonstrated. For this the magnets were placed in series with the discharge and a small transistorized starting circuit was placed between the discharge anode and cathode. The use of rechargeable batteries to power a low-duty cycle thruster and the storage of xenon propellant as a superfluid in lightweight tanks was also studied.

Introduction

The low-power (1 kW or less) magnetoplasmadynamic (MPD) thruster is attractive for auxiliary propulsion applications such as satellite station keeping and attitude control.[1] Good thrust performance (figs. 1 and 2) has been reported for a downstream cathode version of the MPD thruster.[2] For actual missions a number of other features are desirable. Four are considered herein:

(1) Vectoring the thruster exhaust beam with applied magnetic or electric fields

(2) Starting and operating the thruster from a single power supply

(3) Powering the thruster from rechargeable batteries

(4) Storing and transporting the thruster propellant in a lightweight tank and supply system

The ability to vector the exhaust beam is desirable so that the thrust used for station keeping can be alined to act through the spacecraft's center of gravity. Also attitude control can then be implemented with fewer thrusters.

Powering the thruster from rechargeable batteries is desirable so that a low-duty cycle thruster can be used. This significantly lowers the required thruster operating life. The batteries can be charged in parallel at available spacecraft voltage and then switched to series for thruster operation. This yields a simple lightweight power conditioning system if only one power supply is required for thruster operation.

Apparatus and Procedure

Thruster

Fig. 3 is a cut-away view of the thruster tested. The molybdenum anode is approximately 6.6 cm in diameter by 10 cm long. The anode cylinder has a slit along its length. It would otherwise act as a one-turn shorted secondary winding greatly decreasing the effective a.c. inductance of the magnet coils. This would preclude use of the magnet coils in the starting circuit to be described later. The 2 percent thoriated tungsten hollow cathode is 0.318 cm in o.d. by 0.229 cm i.d. by 2.5 cm long. The cathode tip is capped by an orifice plate 0.076 cm thick with a 0.033 cm diam orifice hole. Xenon propellant feed was split for most of the testing, with the majority (80 percent or greater) entering the anode via two feed tubes placed 180° apart and set perpendicular to the anode surface. The remainder of the flow enters the thruster via the downstream hollow cathode.

Two 360-turn edge wound electromagnets were used to produce the magnet field. A set of two 1020 low carbon steel pole pieces were used to shape the field. Like the anode, the pole pieces were slit open along their length and/or radius to prevent power loss in the start-up circuit. Fig. 4 shows the pole pieces, anode and electromagnets, and presents the magnet field plot in iron filings for a commonly used magnetic field current, namely 4 amps to the exhaust end coil and 0 amps to the upstream coil. Additional details of the thruster construction are discussed by Burkhart.[2]

Skewed Coil Thruster

A special version of the above thruster was used for thrust vectoring tests. The exhaust end coil was replaced with the two skewed coils shown in Fig. 5. For these two 100 turn coils, the 10 turn winding layers were interwound at the intersections. The normals to the planes of the coils are each 20° from the thruster center line. The thruster was operated such that the two normals to the coil planes and the thruster center line were in the same geometrical plane. This geometrical plane was placed horizontal for all testing. Vectoring was achieved by unbalancing the currents in the two coils.

Gimbaled Cathode Thruster

The variation of the thrust vector position with cathode position was investigated using a gimbaled cathode thruster. A top view is shown in Fig. 6. Here the cathode is pivoted about an axis in the end plane of the original exhaust end magnet. Cathode deflections of ±20° from axis are possible with this configuration.

Molybdenum Button Probe

Fig. 7 is a sketch of the 0.9 cm diameter molybdenum button probe and the circuitry used to measure the ion flux in the thruster exhaust for thrust vectoring

studies. The probe was mounted on an insulated arm so that its plane could be horizontally traversed through the thruster exhaust at a station 22.5 cm downstream of the exhaust end pole piece (25.4 cm downstream of the intersection point of the two skewed magnets). This horizontal position (actually the radial position relative to the thruster axis) was measured by a linear potentiometer circuit.

"One-Power-Supply" Circuit

Fig. 8 shows the circuit used to achieve "one-power-supply-operation" of the MPD thruster. The two edge wound magnets are placed in series with the positive side of the power supply. A 0.05 μf capacitor is placed around the magnets to limit the peak start-up voltage. The circuit branch in parallel with the thruster is for start-up. The transistor is turned on for 2.5 millisec before ignition is desired. With the power supply set for 200 volts (and no gas flow), the waveform shown in Fig. 9 is generated when the transistor switch is turned off. The peak voltage is given approximately by

$$V_{peak} \simeq \frac{V_{supply}}{R}\sqrt{\frac{L}{C}} \qquad (1)$$

where V_{supply} is power supply voltage, R is the value of resistance in the transistor circuit branch, L is the total inductance of the magnet coils and C is the capacitance of the capacitor parallel to the magnets.

Nude Ionization Gauge

For start-up conditions, the thruster cold flow pressure vs time profile was desired. To achieve this a commercially available nude ionization gauge was mounted on axis between the exhaust end pole piece and the cathode tip, 0.64 cm from the cathode tip. The gauge's collector current was monitored directly on an oscilloscope.

Nickel-Cadmium Batteries

A 168 volt (nominal value) rechargeable nickel-cadmium battery was constructed by placing a 140 sub-C cells (45 g mass per cell) in a single series string. Battery charging was carried out by switching the large series string into seven 20 cell (24 volt, nominal) strings and then charging the seven strings in parallel. For this series of tests the batteries were located outside of the vacuum tank.

Thrust Stand, Thrust Data, and Vacuum Tank

All thrust readings were taken by mounting the thruster on a parallelogram-pendulum thrust stand. The thrust stand displacement is linearly proportional to thrust for small displacements. This displacement is sensed by a linear voltage differential transformer and the conditioned (demodulated) signal is displayed on a strip chart. A series of three calibration weights permit a stand calibration before each reading. More detail on the thrust stand can be found in Burkhart.[2]

For thrust performance, measurements are made of thrust stand deflection, discharge current, discharge voltage, magnet current, magnet voltage, tank pressure, and propellant flow rate. These parameters are then used to calculate specific impulse, thrust efficiency and total efficiency given, respectively by

$$I_{sp} = T/\dot{m}g \qquad (2)$$

$$\eta_T = T^2/2\dot{m}\,P_D \qquad (3)$$

$$\eta = T^2/2\dot{m}\,P \qquad (4)$$

where T is the thrust, $\dot{m}$ the mass flow rate, g the gravitational constant, P_D the power supplied to the discharge and P the total power supplied to magnets and discharge. Propellant mass flow rates are set by varving the pressure upstream of fixed size "calibrated leaks." These leaks were calibrated by a positive displacement flow technique.

Experiments were conducted in a 1.5-m-diam by 5.0-m-long vacuum tank. For all tests the background pressure was maintained at 2.0×10^{-5} torr or less. The thrust stand was mounted at one end of the tank, and the thruster exhaust plume extended along the tank's axis.

Results and Discussion

Thrust Vectoring

In Seikel et al[1] mention is made of the fact that tilting the magnet coil of the upstream cathode MPD thruster caused a visual deflection of the exhaust beam. The skewed coil arrangement of Fig. 5 is an attempt to implement this idea on the newer downstream cathode MPD thruster. In Fig. 5 only one-half of the potential system is shown. In a real system, a second set of coils, rotated 90^o, would be used to provide thrust vectoring in the perpendicular direction. A four coil system would thus provide thrust vectoring at any angle. The turns of the four component coils would be interwound at the 12 points of intersection.

Coil currents of 8.2 amps to each of the two skewed coils of Fig. 5 give a field shape quite close to that of the original edge wound magnet, Fig. 4, and also provides the same flux density vs distance profile on the thruster axis. As the coil currents are progressively unbalanced, the field is progressively bent. One might expect the field vector to tilt a full 20^o when one coil is producing all of the flux and the other coil is completely turned off. But with the configuration of Fig. 5 this does not happen. Magnetic field maps indicate that the pole pieces limit the thruster center line field bending to a maximum of 5^o despite the 20^o coil tilt.

Molybdenum button probe measurements confirmed that the exhaust beam bent the same number of degrees as the thruster center line magnetic field. Hence, the vectoring was also limited to a maximum of $\pm5^o$ for the configuration of Fig. 5.

Typical x-y plotter traces of ion saturation current as a function of radial position are shown in Fig. 10. Left on the traces corresponds to left when looking upstream into the throat of the thruster. The probe was

moved in and out of the plasma a number of times for each data curve. All data showed some degree of non-repeatability at the peaks of the ion flux distribution, but good repeatability on the sides of the distribution. Hence the amount of radial displacement shift, R_{ad}, of the distribution was measured at identical distribution heights approximately 1/2 of the peak value instead of at the peak. Since the axial distance, A_x, from the probe face to the point of intersection of the skewed coils is known, the beam vector angle, α, can be computed from

$$\alpha = \tan^{-1} \frac{R_{ad}}{A_x} \qquad (5)$$

Fig. 10 shows about 3.5^o of shift to the left in the ion flux distribution for a 3.5^o shift to the left in the magnetic field.

The $\pm 5^o$ limit imposed by the pole pieces of the skewed arrangement of Fig. 5 leads one to search for a better location of the skewed coils. Placement of the skewed coils between the exhuast end pole piece (see fig. 3) and the cathode tip appears to be one potentially good location.

Tests of the gimbaled cathode thruster (fig. 6) demonstrated that gimbaling cathode position (electric field) does not produce thrust vectoring. The cathode was rotated from left to right, $\pm 20^o$, with no shift whatsoever in the ion flux distribution. The possiblity of operation with an off-axis cathode is thus feasible. Such cathode locations might be more desireable to improve cathode endurance and life.

Start-up with "One-Power-Supply-Circuit"

The Paschen breakdown characteristic for xenon gas is given by Schönhuber.[3] His experiments were conducted with flat steel electrodes, carefully polished and conditioned before each set of data. Under these carefully controlled conditions, the minimum breakdown voltage is 250 volts at a $p_o d$ product of 6.5 torr-cm. Here p_o is xenon gas filling pressure and d is the distance between electrodes.

With a d.c. input voltage of 200 volts, the circuit of Fig. 8 is capable of generating a peak voltage of 800 volts as shown in Fig. 9. According to Schönhuber's[3] data this should be adequate for breakdown over the $p_o d$ range of 1.5×10^{-1} torr-cm to 2.0×10^{2} torr-cm. The shortest distance between any point on the thruster anode and the cathode tip is 10 cm. Hence under ideal conditions (certainly not present in the MPD thruster) a minimum filling pressure of 1.5×10^{-2} torr would suffice. The steady-state cold flow pressure of the thruster with typical mass flow (0.78 mg/sec to the anode and 0.09 mg/sec to the cathode) is only 5.0×10^{-4} torr. This pressure was sensed by the nude ionization gauge placed 0.64 cm upstream of the cathode tip. As expected, experimentally this pressure is not adequate to ignite the discharge with the 800 volt-peak voltage pulse.

To increase the pressure between the electrodes, a plenum was created in each propellant line by installing solenoid valves between the thruster and the tiny "calibrated leaks" used to control flow. The valves used in these initial experiments were ordinary slow-opening a.c. solenoids. Normal flow rates were used to fill the two plenum chambers, filling time being carefully monitored to determine mass accumulation. The two valves were then "over" driven open in about 10 milliseconds by applying a large current pulse to them. Fig. 11 shows the pressure vs time characteristic achieved when 180 mg of propellant are accumulated in the anode plenum and 180 mg of propellant are accumulated in the cathode plenum prior to valve opening. Time zero is the instant at which the command is given to the valves to open. The pressure peak of 0.29 torr obtained is more than an order of magnitude greater than needed for ignition with 800 volts. And indeed, ignition occurs on the first voltage peak when the transistor switch is opened 22 milliseconds after the valve open command (in other words, at the peak of the pressure pulse).

Over driving these two slow-opening valves to achieve fast opening is undesirable. A valve life of 10 to 15 cycles for these experiments proves this point. Better quality "fast-opening" valves are available. Another improvement would be to reduce the plenum sizes and hence the amount of propellant needed for each starting pulse.

Steady-State "One-Power-Supply-Operation"

Fig. 12 shows the performance achieved at one set of flow conditions when the two edge wound magnets are placed in series with the discharge power. I_{sp} is changed simply by changing the power supply voltage. The figure shows both the thruster efficiency, η_T, and the total efficiency, η, plotted over the 800 to 2200 sec range. The flow and discharge conditions are typical of those used in the experiments of Ref. 2.

A complete set of performance data for this configuration has not been obtained, so Fig. 12 may not represent optimum performance. This series magnet thruster is nevertheless quite good even when magnet power is included. The curves of Fig. 12 are not much worse than the best data with constant magnet current shown in Fig. 1. With additional parametric variations and with better matching of the magnet to the discharge current (achievable by varying the total number of magnet turns) improvement in performance should be attainable. The series magnet arrangement tends to stabilize the discharge. Tendencies to jump into a low-voltage high-current mode are restrained by the series inductors. A further advantage of the circuit of Fig. 8 is that it does not use an external ballast resistor as did the previous configurations.[2] Hence the only external power drain is the thruster discharge and magnets.

Nickel-Cadmium Battery Operation

Battery powered operation of the downstream cathode thruster of Fig. 3 was investigated with the 140 cell battery previously described. In Table 1 are presented the thruster operating parameters measured with this nominal 168 V battery at three different mass flow conditions. For each of these cases, the initial battery voltage was

173 V before loading; the voltage dropped to about 158 volts under load. The 297 watt, 8.8 mN thrust condition is quite close to the 300 watt, 9.0 mN thrust condition of Fig. 2 for which the battery was designed

The 140 cell battery that was tested has a nominal capacity of 202 watt-hours and a mass of 6.3 kg. It was designed for 10 minutes of thruster operation, which corresponds to discharging the battery to a depth of 25 percent. Limiting the depth of discharge to this value permits a larger number of charge-discharge cycles (up to 10 000 for quality batteries).[4,5]

Thrusting at this 8.8 mN level for 10 000 cycles of 10 minutes duration produces a total impulse of 5.28×10^4 N-sec in a total thrusting time of 1667 hours. This for example could provide east-west station keeping for 5 years on a 3500 kg (7700 lbm) synchronous satellite (assume required velocity change of 3 m/sec-yr). Similarly two such thrusters and batteries could provide north-south station keeping for 3 years on a 590 kg (1300 lbm) synchronous satellite (assumed required velocity change of 60 m/sec-yr). For longer missions or heavier satellites, the system would require either a higher performance thruster or proportionally heavier batteries and longer operating time.

These battery operating thruster systems with a low-duty cycle have a number of potential advantages including significant reduction of:

(1) The required thruster operating life

(2) The difficulty of testing to demonstrate thruster reliability

In addition, if the batteries are charged in parallel at spacecraft voltage and then series connected for thruster operation, the batteries plus switching and charging circuits replace a power conditioning system. Since such a battery system would be electrically disconnected from the spacecraft during thruster operation, this system also minimizes any potential electrical coupling between a thruster and its spacecraft.

Xenon Propellant Storage

Lightweight propellant storage for auxiliary propulsion applications has received wide attention including studies by Hughes Aircraft,[6] Frey et al.,[7] and Holcomb.[8] Drawing upon these studies an analysis is made of a xenon propellant tank. The amount of propellant to be stored could vary from 5.5 kg (12 lbm) to 22.0 kg (48 lbm) depending on the mission to be accomplished.

A sperical tank with a wall thickness negligible compared to tank radius is assumed. If R_T is the tank radius, τ the tank wall thickness, ρ_{XE} the storage density of xenon and ρ_T the density of the tank material, then the xenon propellant weight, W_{XE}, and tank weight, W_T are given repectively by

$$W_{XE} = \frac{4}{3}\pi R_T^3 \rho_{XE} \tag{6}$$

$$W_T = 4\pi R_T^2 \tau \rho_T \tag{7}$$

The tank wall thickness required is obtained from a stress balance on the tank wall

$$\tau = \frac{N p_{XE} R_T}{2S} \tag{8}$$

where N is a safety factor, herein assumed to be 2.2, as in Refs. 6 and 7, p_{XE} is the xenon storage pressure and S is the allowable stress, here assumed equal to the yield strength of the tank material.

Combining Eqs. (6), (7), and (8), yields for the tank to propellant weight ratio

$$\frac{W_T}{W_{XE}} = \frac{3}{2}\left(\frac{N\rho_T}{S}\right)\left(\frac{p_{XE}}{\rho_{XE}}\right) \tag{9}$$

Xenon is a highly compressible gas and/or superfluid in the range of storage pressure anticipated (4×10^6 to 15×10^6 N/m^2). Hence, p_{XE}/ρ_{XE} is expressed in terms of the compressibility factor Z as

$$\frac{p_{XE}}{\rho_{XE}} = Z\left(\frac{p_{XE}}{\rho_{XE}}\right)_{\substack{\text{at } 0^oC \text{ and} \\ 1 \text{ atm.}}} \tag{10}$$

Substituting Eq. (10) into Eq. (9) gives the tank to propellant weight ratio in terms of tank material properties (ρ_T and S) and in terms of Z

$$\frac{W_T}{W_{XE}} = \frac{3}{2}\left(\frac{N\rho_T}{S}\right) Z \left(\frac{p_{XE}}{\rho_{XE}}\right)_{\substack{\text{at } 0^oC \text{ and} \\ 1 \text{ atm.}}} \tag{11}$$

Fig. 13 is a plot of the xenon compressibility factor vs propellant storage pressure as taken from Michels et al[9]. Curves are shown for 0° C, 25° C, and 50° C. It is assumed that the spacecraft temperature will be controlled to 25° C, but that it could go as high as 50° C and that design should allow for such possible excursions. The minimum value of Z on the 50° C curve thus minimizes W_T/W_{XE} as given by Eq. (11). The value of Z = 0.511 at a filling pressure of 1.013×10^7 N/m^2 (100 atm) is selected since it corresponds to a data point measured by Michels et al.[9]

Titanium alloy type 6Al-4V is a very frequently used material for propellant tanks.[6,7] Using Eq. (11) the value of $S = 10^9$ N/m^2 and $\rho_T = 4.43\times10^3$ kg/m^3 for Titanium 6Al-4V from Ref. 6, and the xenon density of 5.9 kg/m^3 at 0° C and 1 atm. from Cook[10] gives a $W_T/W_{XE} = 0.13$. From Eq. (10), the density of xenon at 1.013×10^7 N/m^2 (100 atm) is 1.15×10^3 kg/m^3. Hence, using Eq. (6), (8), and (11), the R_T, τ and W_T values can be calculated. Table 2 shows these tank parameters calculated for propellant loads of 5.5 kg and 22.0 kg in a titanium 6Al-4V tank.

If one were to go to a more advanced technology material such as Filament-wound epoxy composite,[6] one might be able to achieve a tank to propellant weight ratio of 9 percent.

The feed system needed for an MPD thruster will be similar to the NH_3 system described by Holcomb.[8] If the propellant tank is cooled lower than 16.6° C, the critical temperature of xenon[10] a liquid phase could develop in the tank. In this event, care must be taken to avoid two phase flow through the flow controlling orifices. This problem, however, is not different than that of a NH_3 propellant system.

Holcomb[8] quotes that 1.38 kg of mass for valving, regulators, vaporizers, filter, etc., are required in a typical NH_3 system in addition to the propellant tankage. A similar value can be assumed for xenon. This 1.38 kg is a fixed weight independent of total propellant loading.

Concluding Remarks

The simplicity of the low-power MPD thruster is one of its attractive features. The studies described herein show that the MPD thruster can be operated with a single power supply. Thrust vectoring, battery operation and lightweight tankage have also been shown to be feasible. Thus, if adequate operating lifetime can be achieved, the low-power MPD arc thruster with a downstream cathode may be attractive for auxiliary propulsion systems.

References

1. Seikel, G. R., Bowditch, D. N., and Domitz, S., "Application of Magnetic-Expansion Plasma Thrustors to Satellite Station Keeping and Attitude Control Missions" Paper 64-677, Aug. 1964, AIAA, New York, N.Y.

2. Burkhart, J. A., "Exploratory Tests on a Downstream-Cathode MPD Thruster," Journal of Spacecraft and Rockets, Vol. 8, No. 3, Mar. 1971, pp. 240-244.

3. Schönhuber, M. J., "Breakdown of Gases Below Paschen Minimum: Basic Design Data of High-Voltage Equipment," IEEE Transactions on Power Apparatus and Systems, Vol. PAS-88, No. 2, 1969, pp. 100-107.

4. Bauer, P., "Nickel-Cadmium Batteries," Batteries for Space Power Systems, SP-172, 1968, NASA, Washington, D.C., pp. 69-128.

5. Robertson, W., Nagle, W. J., and Soltis, D. G., Direct Energy Conversion Division, NASA Lewis, private communication.

6. Anon., "Spacecraft Attitude Control Gas Systems Analysis," SSD-70172R, NASA CR-86661, Apr. 1967, Hughes Aircraft Co., El Segundo, Calif.

7. Frey, J. R., Tyler, J. S., and Burgess, G. A., "Cryogenic Propellant Feed Systems for Electrothermal Engines," AE-1952-R, NASA CR-52151, 1961, AiResearch Mfg. Co., Los Angeles, Calif.

8. Holcomb, L. B., "Satellite Auxiliary-Propulsion Selection Techniques," Tech. Rep. 32-1505, Nov. 1970, Jet Propulsion Lab., California Inst. Tech., Pasadena, Calif.

9. Michels, A., Wassenaar, T., Wolkers, G. J., and Dawson, J., "Thermodynamic Properties of Xenon as a Function of Density up to 520 Amagat and as a Function of Pressure up to 2800 Atmospheres, at Temperatures Between 0° C and 150° C," Physica, Vol. 22, 1965, pp. 17-28.

10. Cook, G. A., Argon, Helium, and the Rare Gases, Vol. 1, Interscience, New York, 1961, pp. 392-393.

Anode flow, mg/sec	Cathode flow, mg/sec	Input power, W	Thrust, mN	I_{sp}, sec	η, %
0.78	0.09	297	8.8	1030	15.0
0.60	0.09	227	6.4	940	12.9
0.78	0.05	256	4.7	570	5.2

TABLE 1 THRUSTER OPERATING PARAMETERS WITH 140 CELL NICKEL-CADMIUM BATTERY

Propellant loading, kg	5.5	22.0
Tank radius, R_T, cm	10.3	16.4
Tank wall thickness, τ, cm	0.115	0.183
Tank mass, W_T, kg	0.71	2.82

TABLE 2 XENON PROPELLANT TANK PARAMETERS-TITANIUM TANK

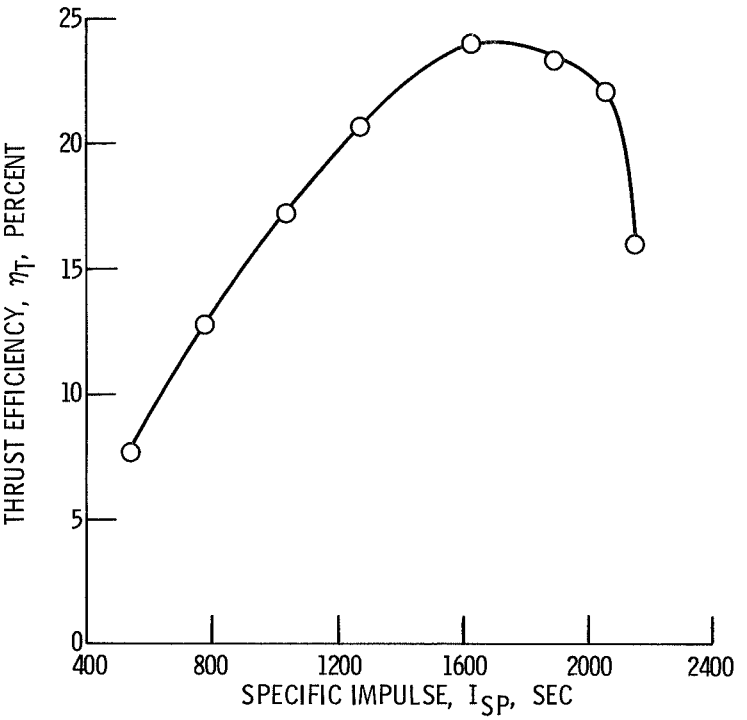

Figure 1. - Thrust efficiency versus specific impulse from reference 2. Total flow 0.78 mg/sec, no cathode flow, and 4 amps to exhaust end magnet. Downstream cathode thruster.

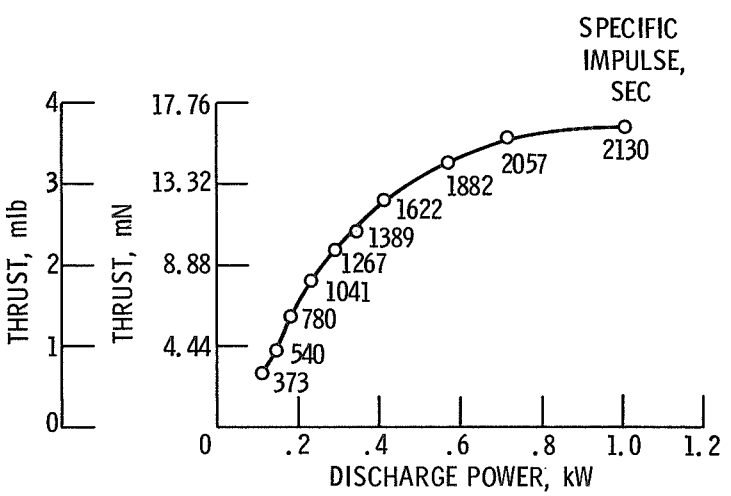

Figure 2. - Thrust versus discharge power for downstream cathode thruster with same conditions as figure 1.

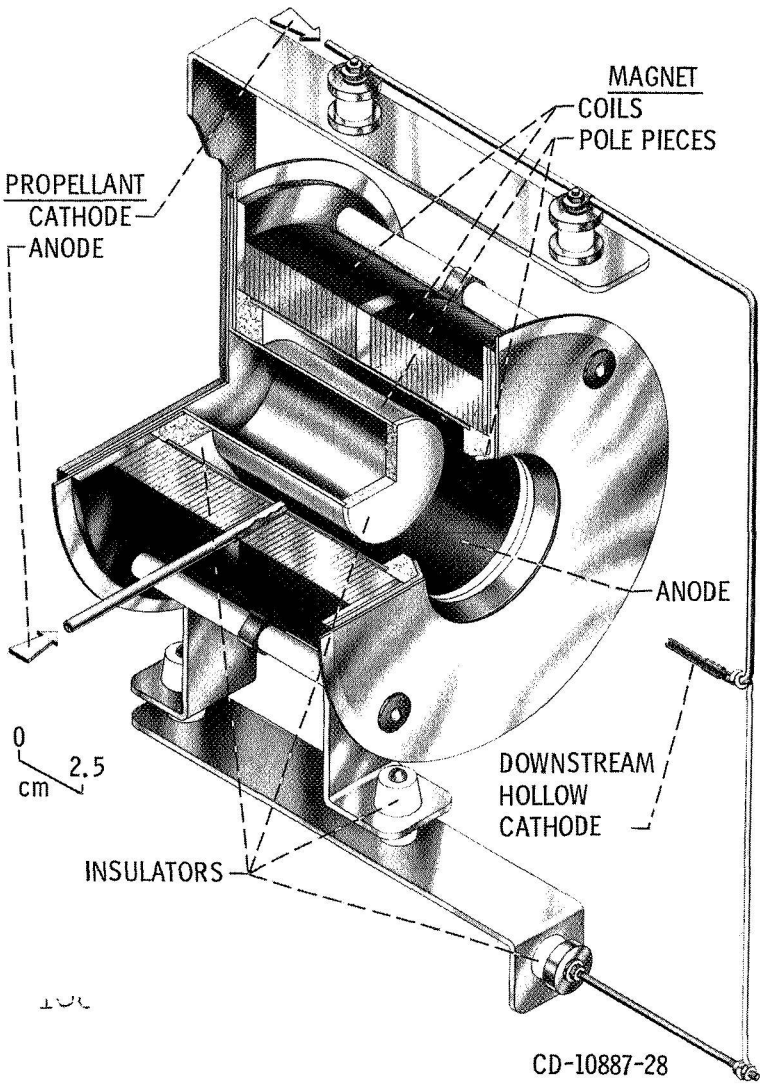

Figure 3. - The downstream cathode MPD thruster.

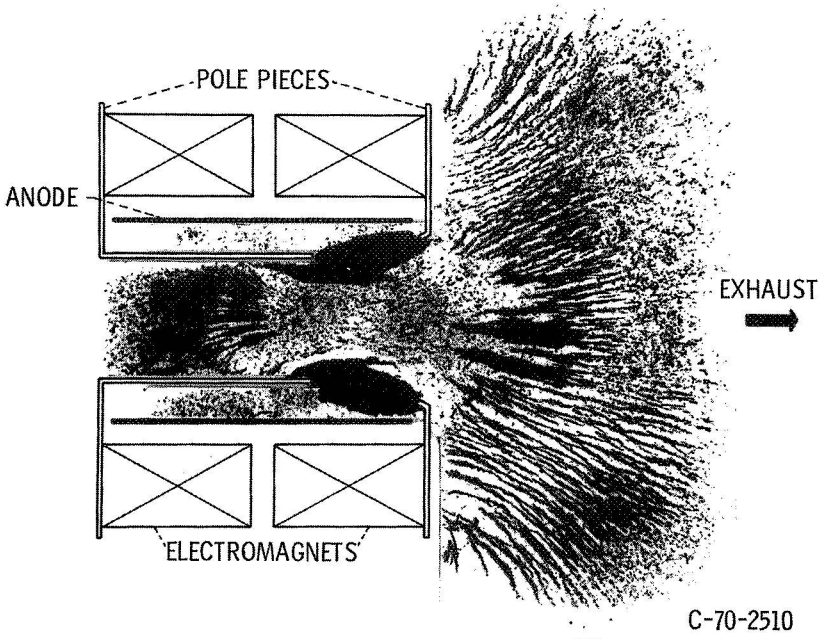

Figure 4. - Magnetic field map of downstream cathode MPD thruster (4 amp exhaust end coil).

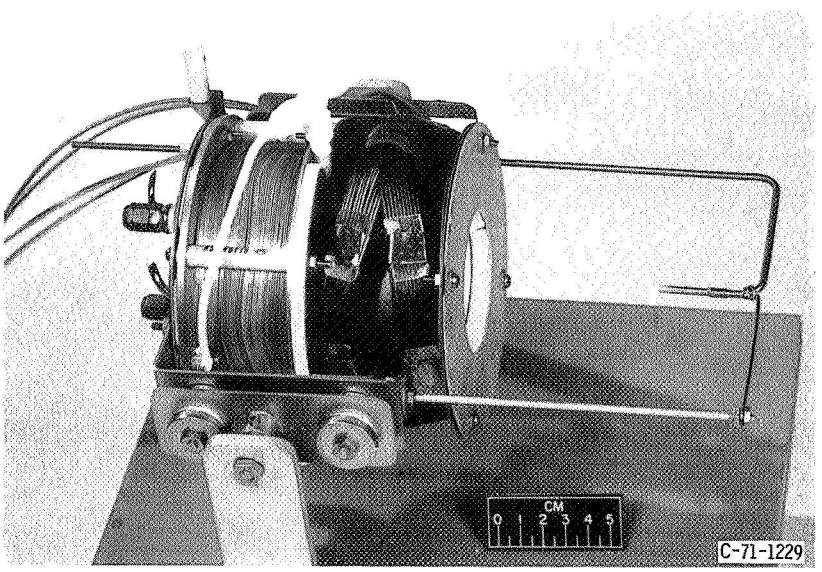

Figure 5. - Skewed coils mounted on MPD thruster in place of exhaust end magnet.

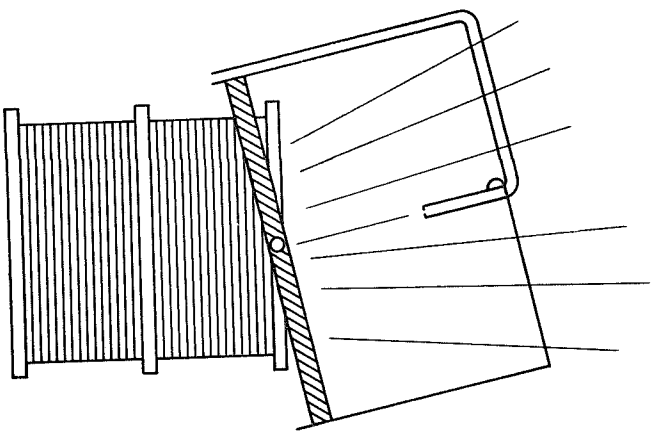

Figure 6. - Gimbaled cathode thruster.

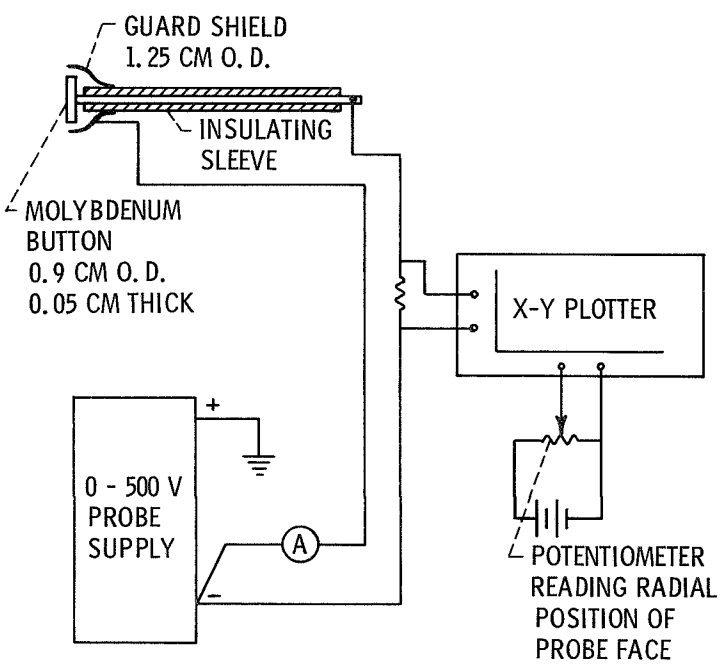

Figure 7. - Molybdenum button probe and circuitry used to measure ion beam flux distribution in MPD thruster exhaust.

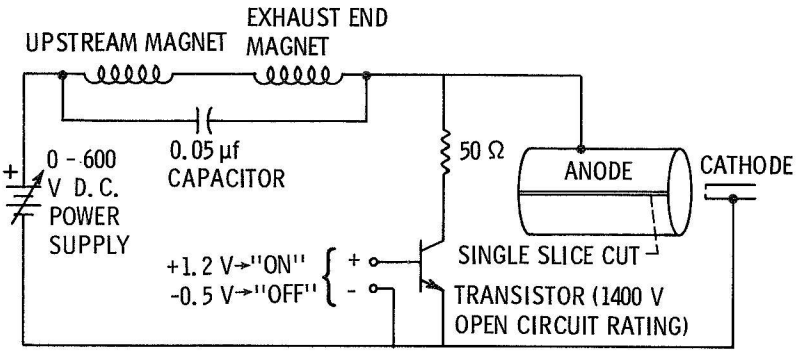

Figure 8. - Circuit used to achieve "one-power-supply-operation" of the MPD thruster.

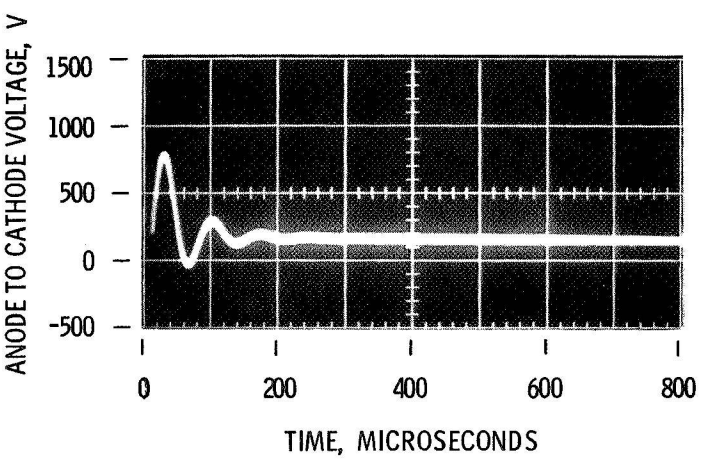

Figure 9. - Anode to cathode voltage. Waveform generated when transistor switch of figure 8 is opened. No gas flow, therefore no-start condition. Power supply set for 200 V d.c..

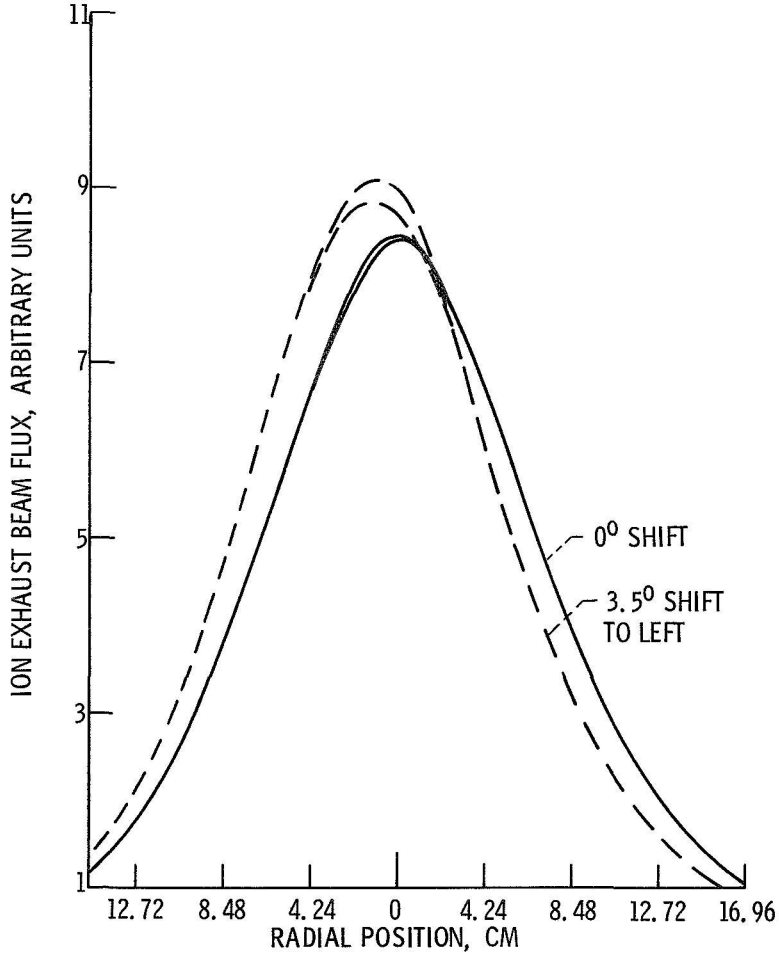

Figure 10. - Plot of ion exhaust beam flux versus radial position, left and right of thruster axis. Thruster operated 0.78 mg/sec anode flow, 0.24 mg/sec cathode flow and 8.2 amps to each skewed coil for 0^{o} shift.

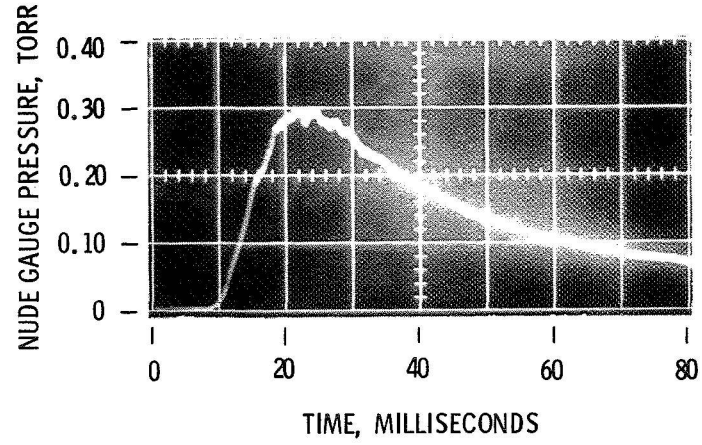

Figure 11. - Plot of pressure vs time sensed by the nude ionization gauge placed between cathode and exhaust end pole piece 0.64 cm upstream of cathode tip. Time zero corresponds to command to open valves.

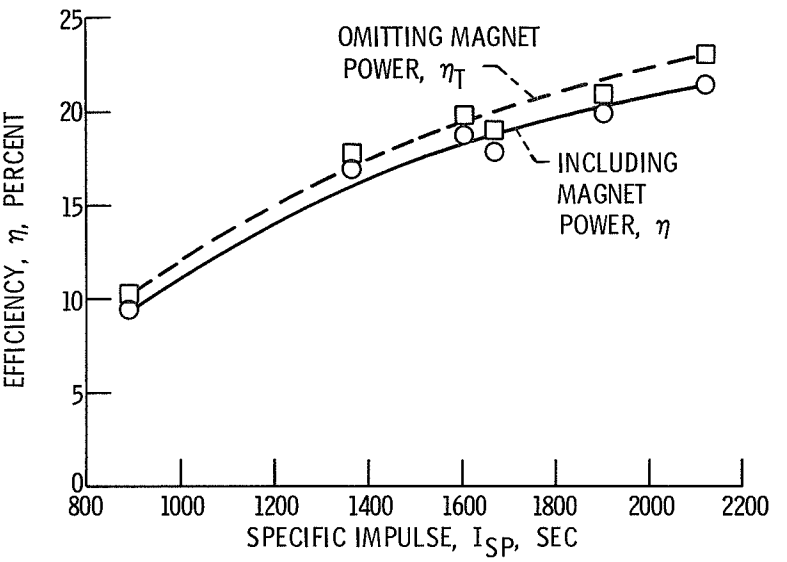

Figure 12. - Thrust efficiency versus specific impulse for both edge wound coils in series with discharge supply. Anode flow 0.78 mg/sec and cathode flow 0.09 mg/sec.

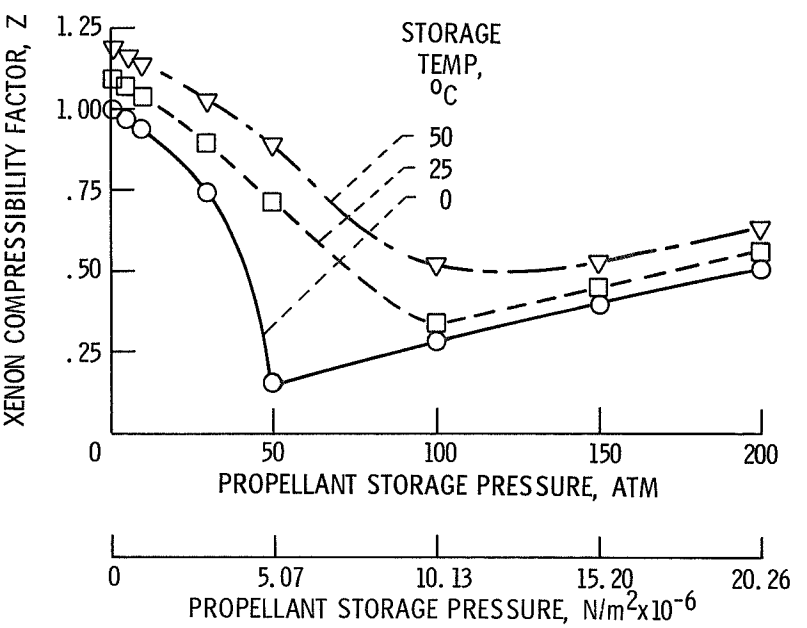

Figure 13. - Plot of xenon compressibility factor, z, as a function of propellant storage pressure with storage temperature as a parameter.